Band-limited exponential correlation function for rough surface scattering

Alongkorn Darawankul and Joel T. Johnson, *Senior Member, IEEE*

***Abstract*— A band-limited exponential correlation function is presented for use in studies of rough surface scattering. This model of surface statistics is developed by multiplying the power spectral density of a standard exponential correlation function surface with a Gaussian roll-off at high frequencies in order to limit the high frequency spectral content of the surface. A parameter is introduced to describe the Gaussian roll-off, and the corresponding correlation function is determined. The primary proposed use of the model is in assessing the contributions of surface high frequency content in the scattering process, particularly in approximate theories of surface scattering. Methods for incorporating this surface description into the standard approximate scattering theories are described, and sample backscattering results provided to illustrate use of the model.**

***Index Terms*— Rough Surface Scattering, Soil Moisture Sensing**

I. Introduction

It is a common practice in studies of soil surface scattering to describe the rough soil surface as a stationary Gaussian random process with an exponential correlation function [1]. Numerous studies have shown both that measured soil surfaces have correlation functions similar to an exponential function, and that measured backscatter data from soil surfaces are often more reasonably modeled using an exponential correlation function. An improved overall understanding of soil surface properties beyond the exponential model has been considered to a lesser degree [2], and, at present, the exponential model remains the most commonly used description in soil surface scattering studies.

A fundamental question common to all models of soil surface statistics involves the accuracy and relevance of their high frequency (i.e. very short length scale) regions. While the exponential surface model includes roughness variations down to arbitrarily small length scales (and also has the associated infinite surface rms slope), true soil surface roughness properties become less meaningful at length scales shorter than the order of 1 mm due to the "clodding" properties of many soil surfaces. Measured soil surface properties have also not been well reported for these length scales. In addition, results described in [3] from a study of 1-D surface scattering suggest that exponential surface length scales shorter than one tenth of the electromagnetic wavelength (in cases where the surface correlation length is larger than the electromagnetic wavelength) have little influence on electromagnetic scattering. However, in a companion work to this paper [4] it is shown for the physical optics theory of rough surface scattering with exponential surfaces that roughness scales even much shorter than the electromagnetic wavelength make a non-negligible contribution to predicted scattered fields. Therefore assessing the influence of the high frequency portion of the surface spectrum on scattered fields remains an important issue for continued studies of soil surface scattering.

Two recent works [5]-[6] have proposed alternative surface descriptions that produce exponential-like correlation functions while varying surface high frequency content, in order to investigate the contributions of surface high frequency components to the scattering process. However the models proposed simultaneously vary other surface properties (such as the slope of the high frequency portion of the surface spectrum) in addition to reducing surface high frequency content, making interpretation of the results obtained less clear.

This work presents a "band-limited" exponential surface model to allow more direct examination of the influence of surface high frequency content on the scattering process. In contrast to previous exponential-like descriptions, the band-limited model is derived simply to truncate the high frequency portion of the original exponential surface at a specified length scale, without varying other properties of the surface. In order to obtain analytical forms for both the surface correlation function and its power spectrum, a Gaussian function is used to perform the truncation; this choice also avoids the oscillations (or sidelobe effects) that would be introduced into the correlation function with other truncation methods. The next section presents the model in terms of both its power spectral density and correlation function. Use of this model in several approximate theories of rough surface scattering is then discussed in Section III. A small set of sample results are illustrated in Section IV in order to demonstrate use of the band-limited surface model in approximate theories of surface scattering. A more detailed study using the model to assess high frequency surface contributions in the physical optics theory is available in [4].

II. The band-limited exponential correlation function

A. Definitions

Begin with the Fourier transform relationship between the surface correlation function $C(x, y)$ and the power spectral

Manuscript received Month dd, yyyy; revised Month dd, yyyy. J. T. Johnson is with The Ohio State University, Dept. of Electrical and Computer Engineering and ElectroScience Laboratory. A. Darawankul was with The Ohio State University, Dept. of Electrical and Computer Engineering and ElectroScience Laboratory, and is now with the A. T. Tri Company.

density $W(k_x, k_y)$:

$$h^2 C(x,y) = \int_{-\infty}^{\infty} dk_x \int_{-\infty}^{\infty} dk_y \; e^{ik_x x} e^{ik_y y} W(k_x, k_y) \quad (1)$$

where h^2 is the surface height variance. This definition and the fact that $C(0,0) = 1$ shows that the power spectral density is normalized so that its integral over wavenumber space is h^2. If we define the Fourier transform operator $\mathcal{F}$ and its inverse $\mathcal{F}^{-1}$ through

$$(2\pi)^2 \mathcal{F}\{q(x,y)\} = \int_{-\infty}^{\infty} dx \int_{-\infty}^{\infty} dy \; e^{-ik_x x} e^{-ik_y y} q(x,y) \quad (2)$$

$$\mathcal{F}^{-1}\{Q(k_x,k_y)\} = \int_{-\infty}^{\infty} dk_x \int_{-\infty}^{\infty} dk_y \; e^{ik_x x} e^{ik_y y} Q(k_x,k_y) \quad (3)$$

then Equation (1) and its inverse can be rewritten as

$$h^2 C(x,y) = \mathcal{F}^{-1}\{W(k_x,k_y)\} \quad (4)$$

$$W(k_x,k_y) = \mathcal{F}\{h^2 C(x,y)\} \quad (5)$$

For surfaces with isotropic statistics (i.e. independent of direction), the correlation function and power spectral density can be written as $C(\rho)$ and $W(k_\rho)$, respectively, where $\rho = \sqrt{x^2+y^2}$ and $k_\rho = \sqrt{k_x^2 + k_y^2}$. Only isotropic surface models are considered in this paper.

Surfaces with an exponential correlation function have

$$C_{\exp}(\rho) = \exp\left(-\frac{\rho}{L}\right) \quad (6)$$

$$W_{\exp}(k_\rho) = \mathcal{F}\{h_{\exp}^2 C_{\exp}(\rho)\} \quad (7)$$

$$= \frac{h_{\exp}^2 L^2}{2\pi}\left(1 + (k_\rho L)^2\right)^{-1.5} \quad (8)$$

where $h_{\exp}$ is the rms height of the exponential surface and L is the surface correlation length, called the "large scale" correlation length in what follows. The k_ρ^{-3} nature of the power spectral density for large k_ρ values results in the unbounded rms slopes of the surface.

As an aside, another recently proposed model of soil surface statistics is the generalized power spectrum model of [7], which has a basic form similar to equation (8) but uses the power of the $\left(1 + (k_\rho L)^2\right)$ term as a parameter. While reference [7] shows that use of the generalized power spectrum model can produce somewhat improved agreement with the measured soil surface scattering data of [8] compared to a true exponential model, the advantages of the generalized power spectrum model remain to be conclusively demonstrated. The generalized power spectrum model is not applicable for the goals of the current study because it does not directly limit the high frequency content of the true exponential surface.

A second Fourier transform pair to be used is that of a Gaussian function:

$$C_{\text{gaus}}(\rho) = \exp\left(-(\rho/L_S)^2\right) \quad (9)$$

$$W_{\text{gaus}}(k_\rho) = \frac{h_{\text{gaus}}^2 L_S^2}{4\pi} \exp\left(-\left(\frac{k_\rho L_S}{2}\right)^2\right) \quad (10)$$

where L_S will be termed the "short scale" correlation length in what follows. Note the power spectral density in the Gaussian case decreases rapidly for $k_\rho > \frac{2}{L_S}$.

B. Band-limited exponential power spectral density

The band-limited exponential power spectral density is defined as a multiplication of the standard exponential power spectral density with a Gaussian roll-off at high frequencies:

$$W(k_\rho) = \frac{h^2 L^2}{2\pi}\left(1 + (k_\rho L)^2\right)^{-1.5} \left[\frac{1}{R}\exp\left(-\left(\frac{k_\rho L_S}{2}\right)^2\right)\right] \quad (11)$$

Constants in the Gaussian power spectral density have been removed in this process, and replaced with the normalization factor R, which will be defined to ensure that the integration over wavenumber yields h^2. Using integral identities from [9] (number 3.369), it can be shown that the normalization factor is

$$R = 1 - q\frac{\sqrt{\pi}}{2}\; e^{\frac{q^2}{4}}\; \text{erfc}\left(\frac{q}{2}\right) \quad (12)$$

where erfc represents the complementary error function [9], and the parameter q is defined as L_S/L. Given the presence of R in the band-limited exponential power spectral density, the low frequency portion of the spectrum is identical to that of a true exponential surface with an increased rms height of $h_{\exp} = h/\sqrt{R}$. Therefore the band-limited surface rms height will be set to $h = h_{\exp}\sqrt{R}$ when comparing with true exponential surface (rms height $h_{\exp}$) properties in what follows.

The Gaussian roll-off factor in equation (11) directly accomplishes the goal of reducing the surface high frequency content while only requiring a single additional parameter, L_S (or equivalently q), for which smaller values shift the truncation point to higher frequencies. Figure 1 is a plot of normalized power spectral densities $W(k_\rho)/W_{\exp}(0)$ (assuming $h = h_{\exp}\sqrt{R}$, $h_{\text{gaus}} = h_{\exp}$, and, for the Gaussian spectrum, $L_S = L$) for varying values of q compared to the true exponential power spectral density. The reduction in high frequency content associated with the Gaussian roll-off is obvious. Figure 2 is a plot of the percent decrease in rms height for the band-limited exponential surface compared to the true exponential surface, i.e. $100\frac{h_{\exp}-h}{h_{\exp}} = 100(1-\sqrt{R})$ versus q. The decrease in rms height becomes small in the true exponential limit $q = 0$, while the overall decrease remains less than approximately 10 percent for q values less than approximately 0.25.

It is also possible to derive the slope variance s^2 of the

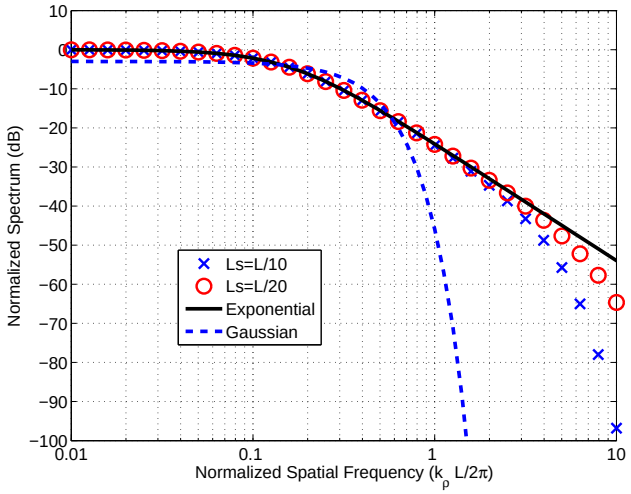

Fig. 1. Comparison of normalized power spectral densities $(W(k_\rho)/W_{\exp}(0)$ assuming $h = h_{\exp}\sqrt{R})$ for Gaussian, true exponential, and band-limited exponential surfaces. The plot horizontal axis is the normalized spatial frequency $\frac{k_\rho L}{2\pi}$.

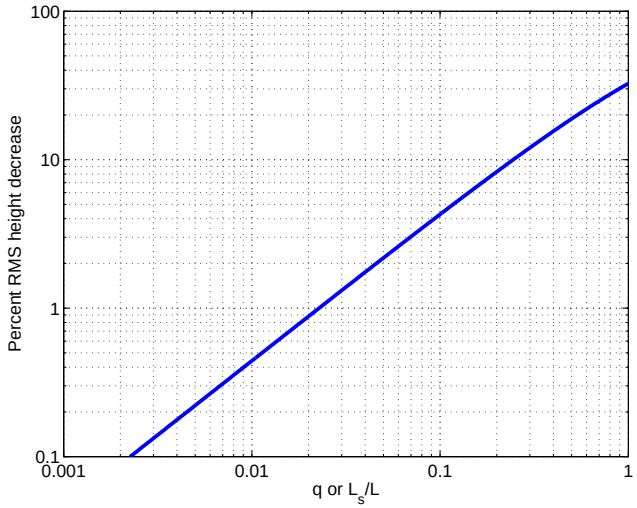

Fig. 2. Percent decrease in band-limited surface rms height compared to true exponential surface $(100(1-\sqrt{R}))$ versus $q = \frac{L_S}{L}$. Note for $q < 0.25$, the decrease is less than 10 percent.

band-limited exponential surface analytically as

$$s^2 = 2\pi \int_0^\infty dk_\rho \; k_\rho^3 W(k_\rho) \tag{13}$$

$$= \left(\frac{h}{L}\right)^2 \frac{\sqrt{\pi}}{qR} \exp\left(\frac{q^2}{4}\right) \left[\left(1+\frac{q^2}{2}\right) \operatorname{erfc}\left(\frac{q}{2}\right) - \frac{q}{\sqrt{\pi}} \exp\left(-\frac{q^2}{4}\right)\right] \tag{14}$$

$$\approx \left(\frac{h}{L}\right)^2 \frac{\sqrt{\pi}}{q} \tag{15}$$

with the last approximation holding as q approaches zero. However, use of this slope variance in a geometrical optics (GO) theory of surface scattering should be performed carefully if L_S is much smaller than the electromagnetic wavelength, since contributions from short scale surface features may not be well modeled by the GO approach [5]-[6]. Further information on the geometrical optics theory for exponential surfaces is provided in [4].

C. Band-limited exponential correlation function

The correlation function for the band limited exponential surface can be found through equation (4). Since $W(k_x, k_y)$ here has been defined in terms of a multiplication of $W_{\exp}$ and W_{gaus}, it is possible to use the convolution property of the Fourier transform in finding $C(x, y)$. The convolution property states that

$$C(x,y) = \frac{1}{h^2}\mathcal{F}^{-1}\left\{AW_{\exp}(k_x,k_y)W_{\text{gaus}}(k_x,k_y)\right\} = \frac{Ah^2}{(2\pi)^2}\int_{-\infty}^{\infty}dx'\int_{-\infty}^{\infty}dy' C_{\exp}(x',y') \; C_{\text{gaus}}(x-x', y-y') \tag{16}$$

where the constant A is found to be $\frac{4\pi}{h_{\text{gaus}}^2 L_S^2}$ by comparing with equations (8), (10), and (11), and where the rectangular coordinate forms of $C_{\exp}$ and C_{gaus} are used.

Transforming the integral in equation (16) into polar coordinates, and again using an integral identity from [9] (no 8.431.3), equation (16) can be simplified to

$$C(\rho) = \frac{2e^{-\frac{\rho^2}{L_S^2}}}{RL_S^2}\int_0^\infty d\rho'\rho' e^{-\frac{\rho'^2}{L_S^2}} I_0\left(\frac{2\rho\rho'}{L_S^2}\right)\exp\left(-\frac{\rho'}{L}\right) \tag{17}$$

where I_0 is the modified Bessel function of the first kind of order zero [9]. If the factor $\exp\left(-\frac{\rho'}{L}\right)$ is expanded in a power series, then another integral identity ([9], no. 6.643.2) and properties of the Whittaker function ([9], no. 9.22) can be used to obtain

$$C(\rho) = \frac{e^{-\frac{\rho^2}{L_S^2}}}{R}\sum_{n=0}^{\infty}\frac{(-q)^n}{n!}\Gamma\left(\frac{n}{2}+1\right) M\left(\frac{n}{2}+1, 1; \frac{\rho^2}{L_S^2}\right) \tag{18}$$

where

$$\Gamma\left(\frac{n}{2}+1\right) = \left(\frac{n}{2}\right)! \tag{19}$$

applies for n even, and

$$\Gamma\left(\frac{n}{2}+1\right) = \sqrt{\pi}\frac{n!!}{2^{\frac{n+1}{2}}} \tag{20}$$

applies for n odd, with $n!! = (n)(n-2)\cdots(1)$. $M(a,b;z)$ in equation (18) is the confluent hypergeometric function of the first kind [10]. This form is expected to converge well when $\rho < L$ due to the series expansion utilized.

While equation (18) may appear complex due to the inclusion of M, in fact, the values of M needed can be evaluated in a recursive process. This is due to the recursion relation [10]

$$M(a,1;z) = \frac{1}{a-1}\left[(2-a)\,M(a-2,1;z) + (2a-3+z)\,M(a-1,1;z)\right] \tag{21}$$

which can be initialized using

$$M(0,1;z) = 1 \quad (22)$$

$$M(\frac{1}{2},1;z) = \exp\left(\frac{z}{2}\right) I_0\left(\frac{z}{2}\right) \quad (23)$$

$$M(1,1;z) = \exp(z) \quad (24)$$

$$M(\frac{3}{2},1;z) = \sum_{m=0}^{\infty} \left(\frac{z}{2}\right)^m \frac{(2m+1)!!}{(m!)^2} \quad (25)$$

For larger values of ρ, asymptotic forms of M [10] can be substituted in equation (18). The series then simplifies considerably, with the result

$$C(\rho) \approx \frac{\exp\left(-\frac{\rho}{L}\right)}{R}\left[1+\left(\frac{q}{2}\right)^2\left(1-\frac{L}{\rho}\right) + \frac{1}{2}\left(\frac{q}{2}\right)^4\left(1-2\frac{L}{\rho}-\left(\frac{L}{\rho}\right)^2-\left(\frac{L}{\rho}\right)^3\right)+\cdots\right] \quad (26)$$

An examination of the convergence of equation (26) shows it to be useful for distances ρ greater than approximately $10L_S$. The near exponential form of the correlation function is obvious in equation (26), along with the influence of q. Note that even at very large values of ρ, the correlation function does become exactly exponential unless q approaches zero.

From equation (26), it is possible to derive the correlation length $L_{\rm bl}$ of the band-limited exponential surface, which is slightly perturbed from that of the true exponential surface L. Use of equation (26) is reasonable for this purpose so long as q is less than approximately 0.25. To second order in q, the true correlation length is

$$L_{\rm bl} \approx L\left(1-\frac{\log(R)}{1-\frac{q^2}{4}}\right) \quad (27)$$

While $L_{\rm bl}$ is the true correlation length of the band-limited surface, it is preferable to continue to express surface properties in terms of the original exponential correlation length L.

In scattering computations, it is the surface covariance function $h^2C(\rho)$ that is utilized; therefore comparisons of covariance functions among surface descriptions are most relevant. The comparison of interest is that of $h^2_{\rm exp}C_{\rm exp}(\rho)$ with $h^2C(\rho)$, which is illustrated in terms of $C_{\rm exp}(\rho)$ and $\frac{h^2}{h^2_{\rm exp}}C(\rho) = RC(\rho)$ in Figure 3 for $q = 0.05$ and $q = 0.1$. A Gaussian correlation function is also shown with $h_{\rm gaus} = h_{\rm exp}$ and $L_S = L$. The figure shows the near-exponential nature of the band-limited exponential case, especially at larger distances from the origin. The Figure inset provides higher resolution near the origin, and demonstrates the limited high frequency content in the band-limited case since the scaled correlation functions show a quadratic behavior as opposed to the linear dependence of the true exponential surface. However the band-limited exponential plots clearly approach the true exponential case near the origin as q is decreased. Note the scaled covariance functions are not required to approach unity at the origin in the band-limited case, due to their normalization by $h^2_{\rm exp}$ instead of h^2. It appears likely that experimental measurements of soil surface correlation functions would be unable to distinguish between the the true exponential and band-limited exponential cases unless extremely high accuracy in the experimental measurement were achieved near the origin of the correlation function.

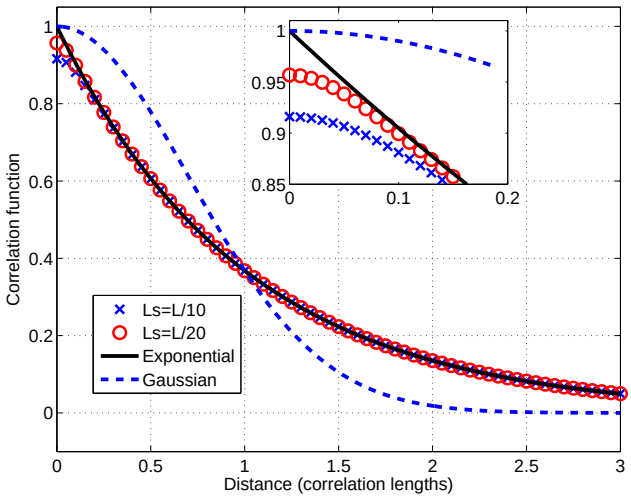

Fig. 3. Comparison of scaled band-limited exponential correlation functions with $q = 0.05$ and 0.1 with true exponential and Gaussian correlation functions.

III. Evaluation of Surface Scattering Models for the Band-Limited Exponential Correlation Function

Numerous approximate theories of rough surface scattering are available [11]; choice of a theory that is most appropriate for a given problem depends on the surface and sensor parameters of interest. In most surface scattering models, the influence of the high frequency portion of the surface spectrum on the scattering process is not immediately obvious, and only repeated computations as the surface high frequency content is varied can be used to investigate this question. Because the band-limited exponential surface model provides a simple means for varying surface high frequency content, it is desirable to assess the use and impact of the band-limited exponential model in these theories.

This issue is considered for a subset of theories, including the small perturbation method (SPM) [1], physical optics (PO) [1], the "integral equation method" analytical model (IEM) [1],[12]-[13], the small slope approximation (SSA) [14]-[16], and the reduced local curvature approximation (RLCA) [17]. Incorporation of the band-limited model into numerical studies of surface scattering is also discussed. A discussion of the geometrical optics (GO) theory for exponential surfaces is provided in [4].

A. Small perturbation method

In the first-order SPM, applicable for small-slope surfaces with small heights and correlation lengths compared to the electromagnetic wavelength, the scattered power is directly proportional to the surface power spectral density evaluated at the Bragg wavenumber (i.e. $k_{\rho,B} = 2k\sin\theta$ for backscattering, where k is the electromagnetic wavenumber and θ is the

incidence angle.) The contribution of high frequency surface content to the scattering process is therefore obvious, and surface length scales shorter than one half the electromagnetic wavelength have no impact on the scattering process.

If scattering from the band-limited exponential surface of rms height $h = h_{\exp}\sqrt{R}$ is to model scattering from a true exponential surface with rms height $h_{\exp}$, we require

$$\exp\left(-\left(\frac{k_{\rho,B}L_S}{2}\right)^2\right) \approx 1 \tag{28}$$

If we replace $k_{\rho,B}$ with its maximum value of $2k$, the above requires $kL_S << 1$. Thus in the SPM limit, L_S must be small compared to the electromagnetic wavelength in order to model scattering from a true exponential surface. The condition required for kL_S is most restrictive for larger Bragg wavenumbers (e.g. backscattering at large incidence angles), and less restrictive for smaller Bragg wavenumbers. For example, using $kL_S = 1$ results in a 4.3 dB reduction in band-limited exponential backscattered incoherent normalized radar cross section (NRCS) values at grazing incidence, but only a 2.2 dB reduction at 45 degrees incidence. Note these specific values are applicable only for small height surfaces.

B. Physical optics and IEM

Both the PO and "single-scattering" IEM theories obtain expressions for the NRCS σ that involve integrations of the form [1]:

$$\sigma \propto \int_{-\infty}^{\infty} dx \int_{-\infty}^{\infty} dy\; e^{-ik_{dx}x} e^{-ik_{dy}y} \left\{ e^{\kappa^2 h^2 C(x,y)} - 1 \right\} \tag{29}$$

where k_{dx} and k_{dy} are the differences between the x and y components, respectively, of the scattered and incident electromagnetic vector wavenumbers, and κ depends on the z components of the wavenumber difference in a manner that is distinct for the PO or IEM theories. It is common in evaluating such integrations to use the expansion

$$e^{\kappa^2 h^2 C(x,y)} = \sum_{m=0}^{\infty} \frac{\left(\kappa^2 h^2\right)^m}{m!} C^m(x,y) \tag{30}$$

so that the required integration can be expressed in terms of a sum involving the Fourier transform of the mth power of the surface correlation function, labeled $W^{(m)}(k_{dx}, k_{dy})$. For the true exponential surface, $W^{(m)}$ can be determined analytically, making evaluation of PO or IEM NRCS predictions possible in terms of a straight forward series summation.

For the band-limited exponential surface, $W^{(m)}$ is not easy to obtain analytically, and the above approach fails. Instead, a direct numerical integration of equation (29) is used (without the series expansion of equation (30)), as is common for other spectral types such as the power-law spectrum model of the sea surface. After a transformation of the integration in equation (29) into cylindrical coordinates, the results simplify into a single integral over the term inside the brackets in equation (29) multiplied by a zeroth order Bessel function of the first kind $J_0(k_{d\rho}\rho)$ and by ρ. Numerical evaluation of this oscillatory integral can be performed by breaking the integration domain into sub-intervals between the zeros of the Bessel function. Doing so allows the numerical integration to be written in terms of a summation of an alternating series of terms (i.e. each sub-integral), the convergence of which can be accelerated using an Euler transformation [18]. The resulting computation remains highly efficient and easily evaluated in seconds for multiple scattering angles with desktop computing resources. The fact that the band-limited surface correlation function is always positive (due to the choice of the Gaussian truncation function) greatly simplifies the resulting algorithm.

Note the IEM model utilized here includes the "transition function" defined in [12]. Though a similar description for backscattering is provided in [13], typographical errors in [13] make use of [12] and [1] preferable. The IEM solution for the backscattered NRCS consists of three terms, each of which requires a separate integration of the form of equation (29).

PO predictions are generally expected to be valid for small-slope surfaces with moderate to large rms heights in terms of the electromagnetic wavelength, and for near-specular angular regions (i.e. near normal incidence for backscattering.) The IEM was formulated to bridge between the PO and SPM theories, and is therefore described as providing accurate predictions for small-slope surfaces of large or small heights compared to the EM wavelength. Due to issues with the IEM for bistatic scattering predictions that have been discussed previously in the literature [11],[19], IEM results are shown only for backscattering. More recent developments of the IEM may remove this limitation, but are not utilized in this paper.

C. SSA and RLCA

Both the SSA and RLCA theories express scattered fields as a series of increasingly complex terms; the basic form of each series term is identical for the SSA and RLCA, but the "kernel" functions involved in each are distinct. Here the contributions of two field series terms are included, resulting in three power terms (i.e. the power in each series term and the correlation between them) included in the NRCS. The first field series term has a form identical to the PO field prediction; in the RLCA the first series term is exactly identical to PO, while in the SSA, the angular function multiplying the PO integral is modified to produce a match to the SPM at first order in the small height limit. The second field series term also involves a PO-like integration, but includes an additional Fourier transform operation inside the integration over surface Fourier coefficients multiplied by an kernel function. When the second field series term is included, the additional Fourier integration results in more complex NRCS equations, so that the computational expense of evaluating SSA or RLCA predictions is larger than that from evaluating PO or IEM predictions. Here the procedure used is based on numerical integration of equations (4)-(6) in [15], using the known correlation function and power spectral density of the band-limited exponential surface. This process requires discretizing the spatial integrals at a rate that is consistent with the high frequency content of the surface; as kL_S is made smaller, finer discretizations (thus more points in the integration) are necessary. In the results to be shown, computational requirements were on the order of ten

seconds for computing the NRCS at a single angle. While this is significantly larger than the PO or IEM requirements, the overall computational load remains reasonable for a desktop computation.

Like the IEM, the SSA and RLCA were formulated to match both the PO and SPM in appropriate limits either for backscattering or bistatic scattering; unlike the IEM, both theories provide a match to the SPM up to second order in the small height limit. While the SSA achieves the high- and low-frequency limits for perfectly conducting surfaces, and the RLCA achieves a match to both PO and SPM for perfectly conducting or penetrable surfaces, it has been shown [15]-[16] that the SSA fails to match the PO for penetrable surfaces. Given this issue and the properties of the IEM, particular attention will be given in the next section to relationships between IEM, SSA, and RLCA NRCS values illustrated.

D. Numerical computations of surface scattering

The strong high frequency content of the exponential surface model is a particular issue in performing Monte Carlo simulations of scattering from true exponential surfaces using the method of moments (MOM) [20]. Because the MOM uses a discretization of the surface profile, a truncation of the high frequency portion of the spectrum is implicit when this discretization is applied. In "point matching" MOM formulations, the surface electromagnetic fields are discretized on the same grid as the rough surface profile, so that the grid must be chosen to resolve both the important roughness features of the surface as well as the variations of the surface fields. The influence of the discretization rate on the MOM is best investigated by truncating the high frequency content of the surface at a fixed cutoff wavenumber less than that of the spatial discretization, and then examining convergence of the resulting fields as the discretization is made finer. Once convergence of the fields is achieved, the process can be repeated with a modified surface spectral truncation point in order to examine the influence of the truncation.

Typically a direct (i.e. rectangular window) truncation of the surface spectrum is used in this process. However it is also typically of interest to compare results obtained from MOM simulations with those obtained from approximate theories of rough surface scattering. Because the latter are simplified through use of the band-limited exponential model, it may also often be desirable to utilize the band-limited model in the MOM. Determination of an appropriate discretization that is sufficient to resolve surface roughness variations is simplified when the band-limited model is used, since surface roughness in length scales much shorter than L_S is greatly attenuated.

IV. Sample scattering predictions using the band-limited exponential correlation function

A. Case considered

Sample results for scattering from band-limited exponential surfaces are illustrated in this section in order to demonstrate use of the band-limited model in the scattering models of the previous section. Further studies providing a more detailed assessment of the influence of surface high frequency content in particular scattering models will be reported in the future; reference [4] provides such a study for the PO. While the results to be shown are limited and primarily consider only a single set of surface statistics, comparison of the predictions of the surface scattering theories considered nevertheless allows some insight into the performance of these models for multi-scale surfaces with truncated high frequency content.

The case considered has $kh_{\exp} = 1.075$, $kL = 6$, and $\epsilon = 4 + i$; these relatively smooth surface statistics were chosen to simplify the numerical computations that will be shown, as well as to be within the expected validity regions of the "advanced" surface scattering models (IEM, SSA, RLCA) while outside those of the classical SPM and PO. The values of kL_S used are either 1 (so that $q = 1/6$ and $kh = 1$) or 0.5 (so that $q = 1/12$ and $kh = 1.036$.) The use of larger kL_S values is useful both in numerical and the SSA and RLCA models, since the required discretization of surface high spatial frequency information is reduced. Note a similar comparison of scattering models for surfaces with Gaussian correlation functions has been reported previously [21].

B. MOM computations

Numerical scattering results were computed using the MOM with the integral equation formulation described in [22]-[23]. Surface sizes were chosen as 32 by 32 electromagnetic wavelengths, sampled into 512 by 512 points, resulting in around one million unknowns (4 unknowns per surface point) for a single surface realization in the Monte Carlo simulation. An iterative matrix equation solution was utilized, and the "canonical grid method" with one series term and a "strong region" diameter of 2.5 wavelengths was used to accelerate required matrix-vector multiply evaluations. Computations were performed for incidence angles of 10, 20, $\cdots$, 50 degrees, and the results to be shown are averages over 80 surface realizations obtained through the use of IBM SP3 parallel computing resources at the Maui High Performance Computing Center [24]. Computations on a single SP3 node for a single realization required approximately 10 CPU hours in order to obtain results for one incident polarization. Additional realizations were included to obtain 152 realizations at incidence angle 50 degrees. Incoherent NRCS values are expected to have converged to within approximately 2 dB for these sets of realizations. The incident field used in the simulations was a "tapered wave" [23] in order to reduce surface edge scattering effects. The tapering parameter $g = 5$ was used, so that the incident field amplitude at surface edges is reduced approximately 54.3 dB compared to that at the center. While this choice of parameters is sufficient to allow reasonable computation of backscattered co-polarized fields at up to 50 degrees incidence, cross-polarized predictions are corrupted by the tapered wave, due to the influence of out-of-plane angular averaging. Therefore, no cross-polarized scattering results are shown in what follows.

C. Results

Figure 4 plots backscattered incoherent NRCS results in both HH and VV polarizations from the MOM for band-limited exponential surfaces with $kL_S = 1$, and compares

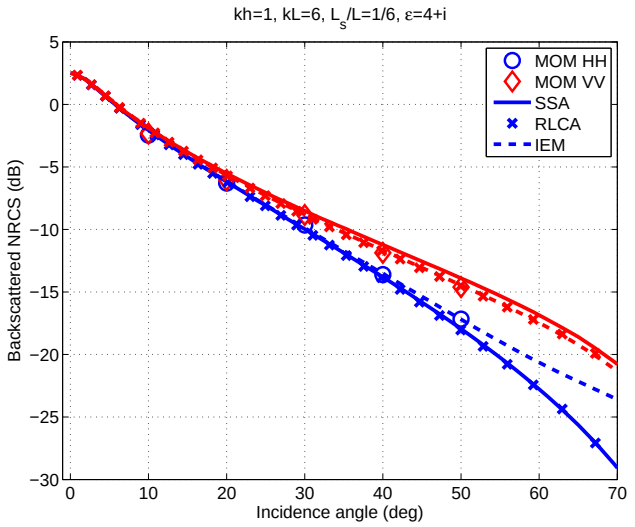

Fig. 4. Comparison of backscattered NRCS values in dB between the MOM, IEM, RLCA, and SSA models, for band-limited exponential surfaces with $kh = 1$, $kL = 6$, $kL_S = 1$, and $\epsilon = 4 + i$

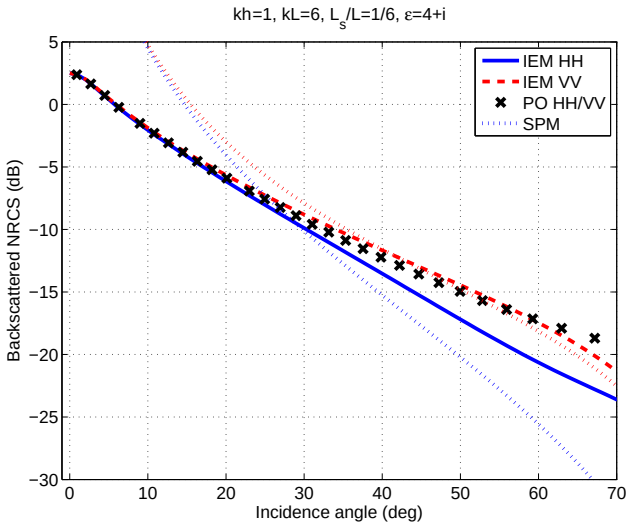

Fig. 5. Comparison of backscattered NRCS values in dB between the IEM, PO, and SPM models, for band-limited exponential surfaces with $kh = 1$, $kL = 6$, $kL_S = 1$, and $\epsilon = 4 + i$

the numerical results with predictions of the IEM, SSA, and RLCA theories. Note the line style in Figure 4 is identical for the HH and VV curves for the approximate theories; however the appropriate polarization can be determined by the fact that all curves closely follow those of the polarization indicated for the MOM results. Results show all theories to yield similar predictions, and to match the MOM reasonably well. The slight differences of any of the theories observed with the MOM are within the error of the Monte Carlo simulation, and therefore no conclusive recommendation of one theory over another is possible based on these results. The small differences observed between the three approximate theories become most pronounced at large incidence angles in HH polarization, where both RLCA and SSA predict much smaller values than the IEM. While the differences between theories are much smaller for VV polarization, the RLCA and IEM models are found to be in close agreement, with the SSA slightly over-predicting their values. Overall, however, Figure 4 illustrates that all three theories appear to be performing reasonably for this case; similar results for Gaussian correlation function surfaces with these parameters were obtained in [21].

Figure 5 illustrates a comparison of the IEM results from Figure 4 with predictions of the SPM and PO. The comparison shows the clear inapplicability of the SPM and PO theories; the former is reasonable only for vertical polarization at large incidence angles, while the latter is useful for near-normal incidence backscattering in either polarization, and for vertical polarization at large incidence angles. Though not included in the Figure, the SSA prediction for HH backscattering at large incidence angles remains significantly larger than that obtained by the SPM.

Figure 6 plots in-plane bistatic NRCS values from the MOM, SSA, and RLCA at 50 degrees incidence angle. The scattering angle of the horizontal axis is defined so that positive 50 degrees is specular scattering while negative 50

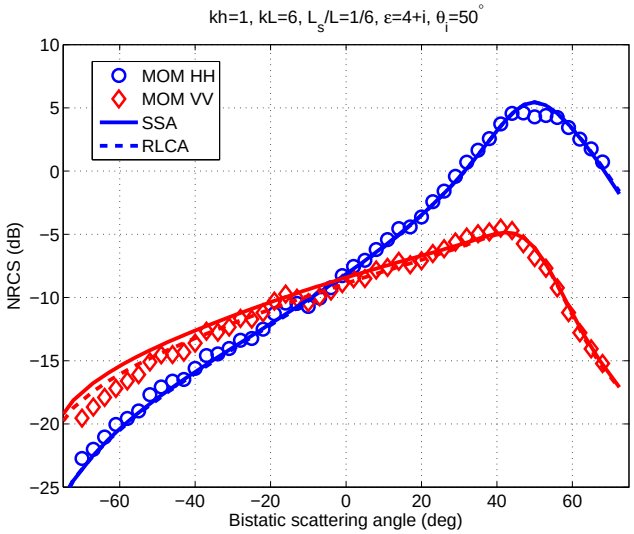

Fig. 6. In-plane bistatic NRCS values in dB for incidence angle 50 degrees; comparison between the MOM, SSA, and RLCA models, for band-limited exponential surfaces with $kh = 1$, $kL = 6$, $kL_S = 1$, and $\epsilon = 4 + i$

degrees is backscattering. Again the results in general show a good match of both the RLCA and SSA to MOM predictions, with much smaller VV returns at positive incidence angles due to a Brewster-angle like effect. The only significant differences observed are at large negative scattering angles in VV polarization, where both methods over-predict MOM results, with RLCA values showing less error. In addition, the slight dip in HH returns near the specular angle occurs due to the influence of coherent scattered field extraction, so that MOM results should not be taken as accurate for this region.

The preceding figures have provided a demonstration of use of the band-limited model in the surface scattering models discussed in Section III, and have shown that the IEM, SSA, and RLCA all provide similar predictions in general agreement with those of the MOM for the particular surface

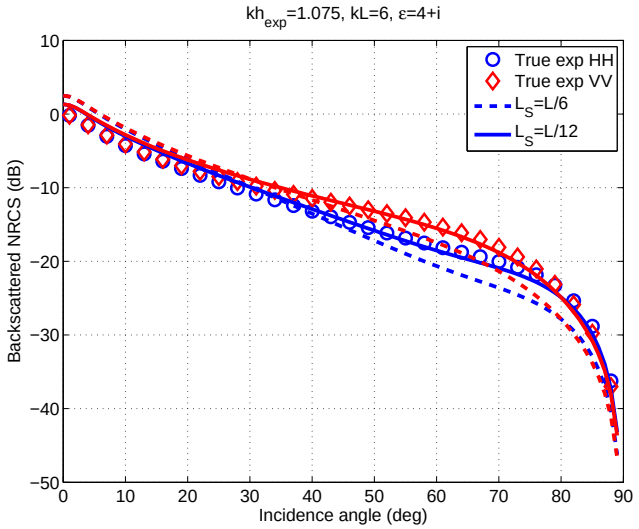

Fig. 7. Comparison of band-limited exponential and true exponential surface IEM backscattered NRCS values in dB as kL_S is varied ,with $kh_{\exp} = 1.075$, $kL = 6$, and $\epsilon = 4 + i$

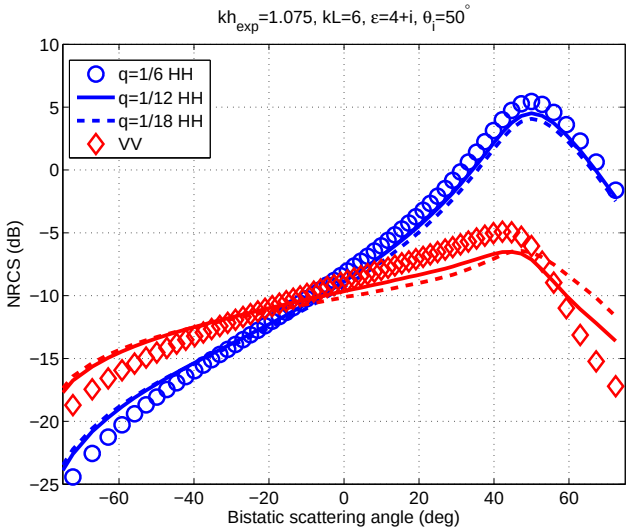

Fig. 8. Effect of q on in-plane bistatic NRCS values for incidence angle 50 degrees with the RLCA model, for band-limited exponential surfaces with $kh_{\exp} = 1.075$, $kL = 6$, and $\epsilon = 4 + i$

statistics investigated. Figure 7 presents a comparison of IEM predictions for band-limited exponential surfaces with those for true exponential surfaces as kL_S is varied from 1 to 0.5. Results show the case $kL_S = 1$ to yield backscattering NRCS values that are significantly larger (around 2.5 dB) than those of the true exponential surface at near-normal incidence angles and significantly smaller than those of the true exponential surface at larger incidence angles. Both of these differences are decreased for $kL_S = 0.5$; in this case, the distinction between the band-limited and true exponential NRCS values is less than 1.5 dB at all angles. The largest differences remain at near normal incidence angles; this is somewhat surprising since it is generally expected that surface high frequency content is less important for near-specular scattering. For the $kL_S = 0.5$ case, the band-limited exponential surface power spectral density at the maximum Bragg wavenumber is reduced by only 1.08 dB compared to the true exponential surface, demonstrating that surface high frequency content is playing a non-negligible role in scattering from the true exponential surface.

Figure 8 explores the influence of q on the bistatic scattering pattern at $\theta_i = 50°$ (as in Figure 6) with the RLCA model. Results are shown for $q = 1/6$, $q = 1/12$, and $q = 1/18$; the latter case has L_s approximately one twentieth of the electromagnetic wavelength. Smaller values of q were not considered in the simulation due to the increased discretization requirements in the RLCA model as discussed in Section III-C. As in Figure 7, the results show a strong influence of surface high frequency content, especially in the forward scattering region of the VV curve.

To study the influence of spectral truncation for surfaces with larger rms heights, IEM computations of normal incidence backscattering were performed with the band-limited model for surface rms heights $h_{\exp}$ ranging from 1 to 10 electromagnetic wavelengths and a correlation length L of ten times the rms height. For each value of the surface statistics, results were computed for L_S ranging from 0.01 to

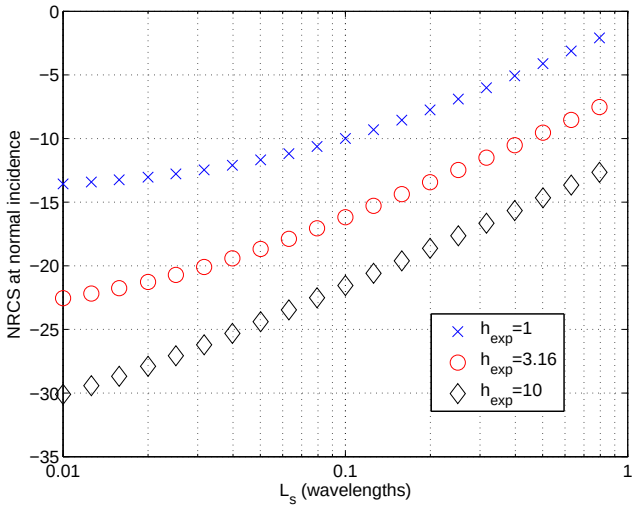

Fig. 9. IEM predictions of backscattered NRCS at normal incidence versus L_S, for specified values of $h_{\exp}$, $L = 10h_{\exp}$, and $\epsilon = 4 + i$

1 electromagnetic wavelength. Figure 9 plots normal incidence backscattered NRCS values for three of the rms height values versus L_S. The curves illustrated all show an increasing trend versus L_S; such an increasing trend is somewhat surprising given the typical expectation that only large scale surface features dominate specular backscattering. However this trend is consistent with the fact that the total surface rms slope is decreased as L_S increases. Note that the $h_{\exp} = 1$ curve shows an apparent saturation at small values of L_S, indicating that roughness features included as L_S becomes less than approximately 0.02 wavelengths are having little impact on the scattering process. No such convergence is observed in the two larger rms height cases however, at least at the level of $L_S = 0.01$ wavelengths. Further discussion of these behaviors is provided in [4].

V. Conclusions

A band-limited exponential correlation function has been derived for studies of rough surface scattering. This model provides a direct limitation of the high frequency content of the true exponential surface, and therefore can be useful in studies of the influence of the high frequency portion of the surface spectrum on the scattering process. In such studies, the analytical form obtained for both the surface correlation function and the power spectral density motivates use of this model in analytical theories of rough surface scattering. Use of the model in several such theories was described, and a simple case was chosen to illustrate example predictions. In the relatively smooth surface case selected, results showed the IEM, SSA, and RLCA models to yield predictions similar to those obtained from the method of moments. A resolution of the small differences between these theories in the case examined will require further numerical simulations. Sample results were also provided to illustrate the importance of surface high frequency content under the IEM and RLCA scattering models. Future studies will attempt to assess more completely the importance of the high frequency portion of the spectrum in the scattering process, as well as the relevance in practice of such high frequency content when describing true soil surfaces. A more detailed study of these issues using the band-limited surface model for the physical optics theory is provided in [4].

VI. Acknowledgments

Helpful discussions with Prof. K. S. Chen of National Central University of Taiwan are acknowledged, as well as the use of IBM SP computing resources at the Maui High Performance Computing Center.

References

[1] A. K. Fung, *Microwave scattering and emission models and their applications*, Artech: Norwood, MA, 1994.

[2] M. W. Davidson, T. LeToan, F. Mattia, G. Satalino, T. Manninen, and M. Borgeaud, "On the characterization of agricultural soil roughness for radar remote sensing studies," *IEEE Trans. Geosc. Rem. Sens.*, vol. 38, pp. 630–640, 2000.

[3] W. Dierking, "Rms slopes of exponentially correlated surface roughness for radar applications," *IEEE. Trans. Geosc. Rem. Sens.*, vol. 38, pp. 1451–1454, 2000.

[4] J. T. Johnson and K. F. Warnick, "On the geometrical optics approximation for scattering for Gaussian and exponential correlated surfaces," submitted to *IEEE Trans. Geosc. Rem. Sens.*, 2007.

[5] A. K. Fung and N. C. Kuo, "Backscattering from multi-scale and exponentially correlated surfaces," *J. Electromag. Waves Applications*, vol. 20, pp. 3–11, 2006.

[6] K. S. Chen, A. K. Fung, J. C. Shi, and H. W. Lee, "Interpretation of backscattering mechanisms from non-Gaussian correlated randomly rough surfaces," *J. Electromag. Waves. Applications*, vol. 20, pp. 105–118, 2006.

[7] Q. Li, J. Shi, and K. S. Chen, "A generalized power law spectrum and its application to the backscattering of soil surfaces based on the integral equation model," *IEEE Trans. Geosc. Rem. Sens.*, vol. 40, pp. 271–280, 2002.

[8] Y. Oh, K. Sarabandi, and F. T. Ulaby, "An empirical model and an inversion technique for radar scattering from bare soil surfaces," *IEEE Trans. Geosc. Rem. Sens.*, vol. 30, pp. 370–381, 1992.

[9] I. S. Gradshteyn and I. M. Ryzhik, *Table of Integrals, Series, and Products, Fifth Edition*, London: Academic Press Inc., 1994.

[10] *Handbook of Mathematical Functions*, M. Abramowitz and I. A. Stegun, eds, Ch. 13 "Confluent Hypergeometric Functions," Dover: New York, 1970.

[11] T. M. Elfouhaily and C. A. Guérin, "A critical survey of approximate scattering wave theories from random rough surfaces," *Waves in Random Media*, vol. 14, pp. R1–R40, 2004.

[12] T. D. Wu, K. S. Chen, J. Shi, and A. K. Fung, "A transition model for the reflection coefficient in surface scattering," *IEEE Trans. Geosc. Rem. Sens.*, vol. 39, pp. 2040–2050, 2001.

[13] A. K. Fung and K. S. Chen, "An update on the IEM surface backscattering model," *IEEE Geosc. Rem. Sens. Letters*, vol. 1, pp. 75–77, 2004.

[14] A. G. Voronovich,, *Wave scattering from rough surfaces*, ser. Springer Series on Wave Phenomena. Springer, 1994.

[15] M. S. Gilbert and J. T. Johnson, "A study of the higher-order small-slope approximation for scattering from a Gaussian surface," *Waves in Random Media*, vol. 13, pp. 137–143, 2003.

[16] C.-A. Guérin and M. Saillard, "On the high-frequency limit of the second-order small-slope approximation," *Waves in Random Media*, vol. 13, pp. 75–88, 2003.

[17] T. Elfouhaily and J. T. Johnson, "A new model for rough surface scattering," accepted by *IEEE Trans. Geosc. Rem. Sens.*, 2006.

[18] Press, W. H., S. A. Teukolsky, W. T. Vetterling, and B. P. Flannery, *Numerical Recipes: The Art of Scientific Computing*, second edition, Cambridge Univ. Press, New York, 1992.

[19] J. L. Alvarez-Perez, "An extension of the IEM/IEMM surface scattering model," *Waves Random Media*, vol. 11, pp. 307–329, 2001.

[20] L. Zhou, L. Tsang, V. Jandhyala, Q. Li, and C. H. Chan, "Emissivity simulations in passive microwave remote sensing with 3-D numerical solutions of Maxwell equations," *IEEE Trans. Geosc. Rem. Sens.*, vol. 42, pp. 1739–1748, 2004.

[21] H. T. Ewe, J. T. Johnson, and K. S. Chen, "A comparison study of surface scattering models," *IEEE Geoscience and Remote Sensing Symposium*, conference proceedings, 2001.

[22] J. T. Johnson, R. T. Shin, J. A. Kong, L. Tsang, and K. Pak, "A numerical study of ocean polarimetric thermal emission," *IEEE Trans. Geosc. Rem. Sens.*, vol. 37, pp. 8–20, 1999.

[23] J. T. Johnson and R. J. Burkholder, "Coupled canonical grid/discrete dipole approach for computing scattering from objects above or below a rough interface," *IEEE Trans. Geosc. Rem. Sens.*, vol. 39, pp. 1214-1220, 2001.

[24] Maui High Performance Computing Center (MHPCC) website, `http://www.mhpcc.hpc.mil`, 2006.